26th EPS Conf. on Contr. Fusion and Plasma Physics, Maastricht, 14 - 18 June 1999 ECA Vol.23J (1999) 1445 - 1448

Dependence of Energy Confinement on the H-mode Pedestal Temperature

G. Janeschitz[1], Yu Igitkhanov[1], M. Sugihara[1]
A. Hubbard[2], Y. Kamada[3], J. Lingertat[4], T. Osborne[5], W. Suttrop[6]

[1]*ITER Joint Central Team, Joint Work Site, D-85748 Garching, Germany*
[2] *Plasma Fusion Centre, MIT, Cambridge, MA 01239, USA*
[3] *JAERI, Naka Fusion Research Establishment, Ibaraki-ken, 311-01 Japan*
[4] *JET Joint Undertaking, Abingdon Oxon., OX14 3EA, UK*
[5] *General Atomics, P.O. Box 85608, San Diego, CA 92186-5608 USA*
[6]*Max-Planck-Institut für Plasmaphysik, EURATOM Assoc., D-85748 Garching, Germany*

1. Introduction: Results published from ASDEX-UP and C-mod show a relation between energy confinement and the temperature on top of the H-mode pedestal (Figs 1,2). This relation can be explained by the observed stiffness of ion and electron temperature profiles (edge and central temperatures are proportional) in both devices [1,2]. Other machines such as JET, DIII-D and JT-60U generally do not report a relation between confinement and pedestal temperature (T_{ped}) which exceeds the contribution of the energy stored in the pedestal itself. However, in some cases (at high density or strong gas puff) a degradation of the energy confinement significantly stronger than explained by the change in pedestal energy occurs also in these machines. This strong confinement degradation can be linked to the relatively low pedestal temperatures in these particular discharges and to the resultant appearance of stiff temperature profiles. (Figs.5-8).

In this paper we propose a possible explanation for the different observations, based on the assumption that both ion and electron thermal diffusivity are strongly non-linear and are governed by turbulence which sets in at a critical temperature gradient [3,4,5]. In cases where energy equipartition between ions and electrons is significant (e.g. at medium to high density and / or at higher Z_{eff}) one would expect that the confinement behavior will be defined by the species having the larger transport.

If ion energy transport is governed by ITG turbulence [4], which brings about a temperature profile stiffness, the energy transport in the ion channel should depend strongly on the H-mode pedestal temperature. Thus in situations for which the ion transport channel dominates stiff temperature profiles will occur leading to a dependence of energy confinement on T_{ped}.

We assume that electron energy transport is also governed by a critical temperature gradient driven turbulence (e.g. Rebut-Lallia-Watkins model [5]). However, in this case the critical temperature gradient has a dependence which does not generate stiff temperature profiles. Therefore the dependence of energy confinement on the pedestal temperature disappears in cases when electron energy transport dominates.

The scaling of the "Turning Point Temperature (TPT)" (i.e. the minimum pedestal temperature (T_{ped},) for which the temperature profile stiffness disappears and energy confinement becomes independent of T_{ped}), can be identified by comparing the critical gradients defined by the two transport mechanisms for electrons and ions, respectively. In this paper a simplified analytic approach using an ITG model [4] and a modified RLW model [5] allows to estimate these TPTs for different machines. The results are compared with the multi-machine "ITER pedestal database".

2. Model and Assumptions: Several assumptions are needed to estimate the TPT with an analytic model: First we assume infinitely strong energy equipartition between ions and electrons (Ti = Te). Second we assume an average shear value of 1.5 in the core plasma for all machines (2 for C-mod) in order to generate critical gradients according to [4] which are large enough to fit the experiments. Third we use radially averaged critical temperature gradients. Fourth we assume that the temperature gradients always follow the critical gradients, i.e. the increase of transport near the critical gradients is much stronger than reported in [4,5] while below the critical gradient neoclassical and superclassical [6] transport is assumed for ions and

electrons, respectively. A stronger increase of transport than in [4,5] when exceeding ∇T^{crit} is required to explain the observed confinement behavior. This assumption can be justified by an avalanche effect when ∇T^{crit} is exceeded [7].

2.1 Ion transport: The critical ion temperature gradient in an ITG model can be written as $\nabla T_i^{crit} \approx T_i f(s,R,q,\nu_*,\tau,L_n)/R$ [4], where f is a function of: shear, q, collisionality, major radius, ion to electron temperature ratio and the density gradient length. If ∇T_i is forced to stay close to ∇T_i^{crit} by a strongly enhanced turbulent transport when $\nabla T_i > \nabla T_i^{crit}$ temperature profile stiffness, ($\nabla T_i \propto T_i$) results, the temperature profile shape is logarithmic and edge and central temperature are proportional (Fig.3,4). Assessing the effective thermal conductivity in the ion channel for a given heat flux q_i as $\chi_{i,eff}^{ITG} \propto q_i / \nabla T_i^{crit}$ and assuming that $\chi_i >> \chi_e$, yields an energy confinement time:

$$\tau_{E/H}^{i} \approx \frac{a^2}{\chi_i + \chi_e} \approx \frac{a^2}{\chi_{i,eff}^{ITG}} \propto \frac{a^2}{q_i}\left(\nabla T_i^{crit}\right) \propto T_{i,}ped\,,$$

As already mentioned this dependence of τ_E *vs. Tped* is actually experimentally seen in all machines in case of low to medium H-mode pedestal temperatures (high density) (Fig. 1,2,5-8).

2.2 Electron transport: In order to explain the experimental observations the transport model chosen must also be governed by turbulence, which sets in at some critical temperature gradient. This critical gradient should display similar dependencies on the main plasma parameters as the L-mode or H-mode scaling relations. A candidate model for ∇T_e^{crit} is therefore the RLW model [5] $\nabla T_e^{crit} \approx \left(\frac{JB^3}{pT_e}\right)^{1/2}$ p - electron pressure, J - current and B - magnetic field.

This model, in contrast to the ITG model, does not produce stiff temperature profiles. It yields a parabolic temperature profile shape (Fig.3,4) and a very weak dependence of energy confinement on the pedestal temperature. The expression for the energy confinement time based on this model is: $\tau_E^e \propto \nabla T_e^{crit} \propto \frac{1}{q}\left(\frac{I_p B^3}{ka^2 n T_e^2}\right)^{1/2}$ yielding: $\tau_{E/H} \propto \frac{R}{\sqrt{P}} I^{0.75} B^{0.25} n^{0.25} k^{0.25}$ which displays the required rough similarity to the dependencies in the L-mode (or H-mode) scaling relations**.**

2.3 Interplay of ion and electron transport and TPT: Let us now consider a hypothetical density scan in H-mode from high density (low T_{ped}) to low density (high T_{ped}) assuming that the density profile is relatively flat, that the pressure on top of the pedestal is constant, i.e. a constant pedestal width with a pressure gradient limited by the ballooning limit, and that predominantly the ions are heated (e.g. NBI). At high density (low T_{ped}), ∇T_i will be limited by a relatively low ∇T_i^{crit} while the critical gradient for electrons is well above the one for ions (1/T dependence) and the electron transport is assumed superclassical [6]. Due to equipartition the electrons are heated by the ions yielding ∇T_e which images more or less ∇T_i. Therefore in this range of pedestal temperatures both the ion and electron temperature profiles appear to be stiff and τ_E increases with increasing T_{ped} i.e. decreasing density (Figs. 1,2 and 5-8 at low T_{ped}).

With further decreasing density T_{ped} rises yielding an increasing ∇T_i^{crit} which eventually will exceed the critical gradient for the electrons. At this point the increase in T_e (due to equipartition) will be limited by ∇T_e^{crit}. The strong equipartition between ions and electrons forces now the ion temperature profile to image the electron temperature profile and thus the ions will not reach their critical temperature gradient. This will cause energy transport being dominated by the electron channel and thus non stiff temperature profiles for electrons and ions as well as a very weak dependence of energy confinement on the pedestal temperature result. Due to the similarity of the dependencies between the RLW related model and the L-mode scaling relation (ITER89P) the energy confinement saturates at an H-factor of ~2 (Figs 5-8 at high T_{ped}). The change from ion to electron dominated energy transport and thus the loss of profile stiffness

happens when $\nabla T_e^{crit} \approx \nabla T_i^{crit}$ averaged radially. Keeping in mind that the density profile in H mode is typically rather flat, the scaling for the TPT (T^*) can be estimated as:

$T^* \propto \sqrt{L_{Ti}} \cdot \left(\frac{I_p B^3}{k a^4 n} \right)^{1/4} \sqrt{\frac{R}{a}}$ where k is an elongation, and L_{Ti} is the T_i gradient length [4].

3. Comparison of the model to the pedestal database and discussion:

Based on the above model the TPT values and the increase of τ_E with T_{ped} were estimated for the specific plasma parameters of each discharge stored in the multi machine "ITER pedestal database" (see also [3]). In Figs. 1,2 and 5-8 the H-factor (normalized to ITER89P) versus T_{ped} is shown for each discharge together with the predicted range of the TPTs represented by a horizontal bar. As one can see the agreement of the predicted and experimentally observed change of confinement behavior is reasonably good. One can also see that there is a range of T_{ped} where the energy confinement saturates at 2 times ITER89P. This is due to the specific dependencies of the two transport models on the plasma parameters. An additional preliminary study of the above transport model using a 1 D code confirmed the results of the analytic model demonstrating that realistic energy equipartition together with the above transport models for electrons and ions, respectively, can reproduce the observed energy confinement behavior.

Another indication that the two transport models above are representative for the physics of ion and electron energy transport is the change of the pressure profile shape observed in a JET density scan during H-mode [9] (Figs 3,4). The density profiles in the core of JET are rather flat, thus the pressure profiles are representative for the temperature profile shape. Due to the different dependencies of ∇T^{crit} on the local temperature one would expect differently shaped temperature profiles (logarithmic versus parabolic) for ion and electron dominated transport, respectively. In addition proportionality of edge and central T in the case when the ion channel governs energy transport is expected. The pressure profiles in Figs 3,4 do show exactly this behavior, i.e. for low density (high T_{ped}, labeld as Type I) we see a parabolic shape (Fig 3) and no proportionality between edge and central pressure (Fig. 4) while for high density (low T_{ped}, labeled as Type III) we see a logarithmic shape (Fig. 3) and a proportionality between edge and central pressure (Fig. 4)

When energy equipartition between electrons and ions is weak and the external sources heat predominantly the ions (NBI), the ion transport would be free to improve beyond the normally limiting electron transport with increasing T_{ped}. Then the energy confinement should also improve significantly above 2 times ITER89P. This is in fact the case in Hot-ion-H-modes where ion heating dominates, a very high pedestal temperature is achieved and a decoupling of electrons and ions in the core plasma as well as a confinement above the standard H-mode can be observed. On the other hand when electrons are predominantly heated and equipartition is weak one should expect a confinement significantly better than L-mode. This is actually also observed in limiter discharges in TORE SUPRA [8] as well as in FTU during LH heating where reasonable agreement with the RLW sacling is seen.

Finally the above considerations are also able to explain qualitatively the good confinement in RI-mode discharges where a peaked ion density profile stabilizes ITG turbulence instead of T_{ped} and thus allow access to regimes where electron transport dominates (IOC, RI-mode, CDH).

References:

[1] O. Gruber,et al., 17th IAEA Fusion Energy Conference, Yokohama (1998), IAEA-F1-CN-69/OV4/3.
[2] M. Greenwald et al., Nuclear Fusion **37** (1997) 793.
[3] G. Janeschitz et al., ITER MEMO Feb.1999, IDoms Nr. G17MD126 99-02-19W0.1.
[4] M. Kotchenreuter et al. Phys. Plasmas 2, 2381 (1995)
[5] P. Rebut, P. Lallia, M. Watkins, IAEA, Proc. 12th Int.Conf., Nice, 1988, p.191;
[6] B. Kadomtsev, "Tokamak plasma: A complex physical system", Plasma series, Inst. of Physics Publishing, Bristol and Philadelphia, 1992
[7] P. Diamond and T. Hahm, Phys. Plasmas 2, 10 Oct. 1995
[8] G. T. Hoang, et.al., Nucl. Fus., Vol. 34, No. 1, (1994)
[9] G. Saibene, et.al, to be published in Nucl.Fus. 1999

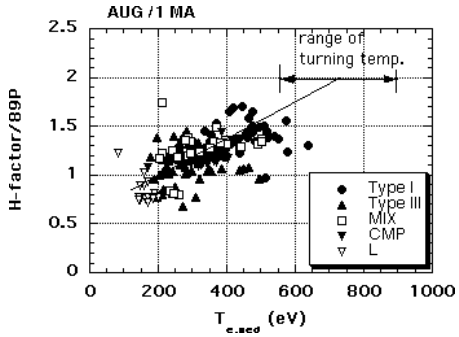

Fig. 1: H-factor (normalized to ITER 89P) vs T_{ped} for 1 MA H-mode discharges in ASDEX-UP. The relation between T_{ped} and confinement can be seen. ASDEX-UP should be always in the stiff temperature profile regime (estimated TPTs higher than experimental T_{ped})

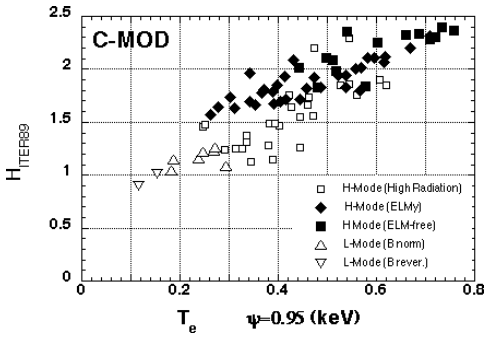

Fig. 2: H-factor vs $T_{q95\%}$ for H-mode discharges in C-mod [2]. Due to the lack of data in our database the estimated TPTs cannot be compared to the above data. However, the estimated TPTs are in most cases higher than T_{ped} explaining the observed profile stiffness.

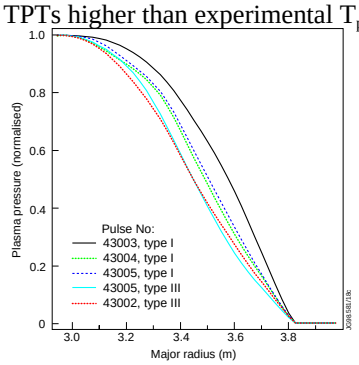

Fig.3: Pressure profiles for a density scan in H-mode in JET calculated by TRANSP [9]. The change from parabolic to logarithmic shape with increasing density (Type III is high density) can be seen.

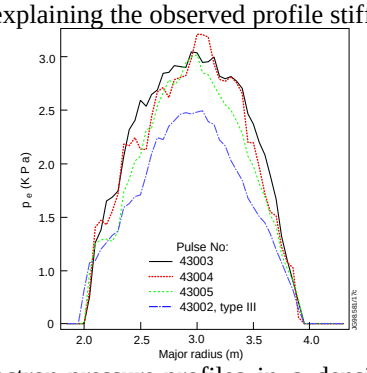

Fig.4: Electron pressure profiles in a density scan in H-mode in JET measured by LIDAR [9]. The proportionalty between edge and central temperature in case of high density (type III) can be seen.

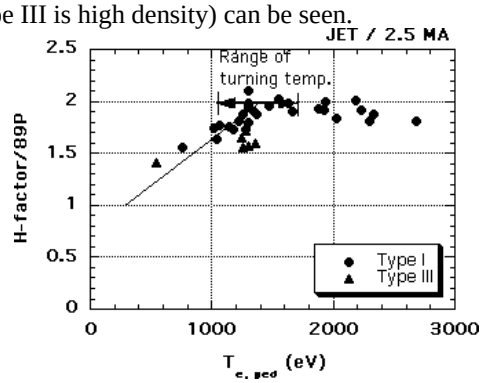

Fig. 5: H-factor vs T_{ped} for 2.5 MA H-mode discharges in JET. The predicted range of TPTs agrees well with the experiment.

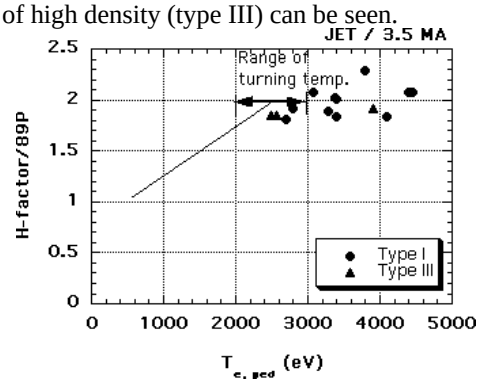

Fig.6: H-factor vs T_{ped} for 3.5 MA H-mode discharges in JET. The predicted range of TPTs agrees well with the experiment.

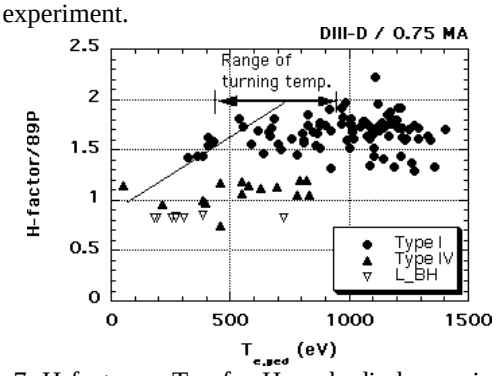

Fig. 7: H-factor vs T_{ped} for H-mode discharges in DIII-D. Large data scatter but again the estimated TPTs agree rather well with the data.

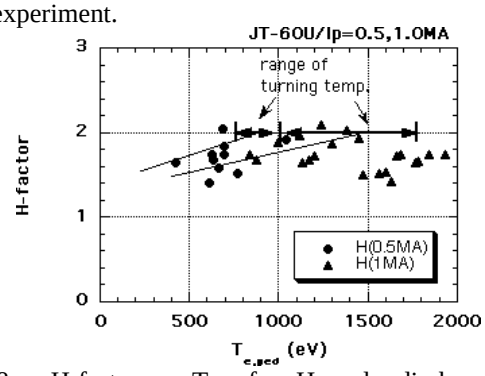

Fig.8: H-factor vs T_{ped} for H-mode discharges in JT60U. Again good agreement between estimated TPTs and data for both plasma currents.